

A feasibility study on active solar space heating technology for office buildings in Greece

Estudo de viabilidade sobre tecnologia de aquecimento solar ativo para escritórios em Grécia

Letiane Benincá(1); Daniel Cóstola(2); Evangelos kyrou(3)

1 Mestre. Universidade Federal do Rio Grande do Sul (UFRGS – Porto Alegre) e Faculdade Meridional (IMED – Passo Fundo). Brasil.

E-mail: letiane.beninca@imed.edu.br

2 Pós-Doutor. Faculdade Meridional (IMED – Passo Fundo) e Starthclyde University (Glasgow, Escócia). Brasil.

E-mail: daniel.costola@gmail.com

3 Mestre. Starthclyde University (Glasgow, Escócia). Escócia.

E-mail: e.kyrou@tue.nl

Revista de Engenharia Civil IMED, Passo Fundo, vol. 4, n. 2, p. 89-109, Jul.-Dez. 2017 - ISSN 2358-6508

[Recebido: Nov. 17, 2017; Aceito: Dez. 04, 2017]

DOI: <https://doi.org/10.18256/2358-6508.2017.v4i2.2281>

Endereço correspondente / Correspondence address

Letiane Benincá

Avenida Brasil, 150 apto 604, Centro, Passo Fundo / RS,

Brasil

CEP: 99010-000

Sistema de Avaliação: *Double Blind Review*

Editor-chefe: Luciana Oliveira Fernandes

Como citar este artigo / How to cite item: [clique aqui/click here!](#)

Resumo

Este artigo explora a viabilidade de utilizar coletores solares térmicos com capacidade de armazenamento e radiadores convencionais para aquecimento de edifícios de escritórios na Grécia. Um modelo dinâmico de simulação na ferramenta ESP-r é utilizado para analisar o desempenho do sistema de coleta solar integrado ao edifício para diferentes perfis de demanda em todas as zonas climáticas da Grécia. O impacto da capacidade do sistema de armazenamento, da área do coletor e do ângulo de inclinação foram investigados quanto ao desempenho geral do sistema. Os escritórios na Grécia se enquadram em vários cenários de demanda de aquecimento anual, determinados pela orientação do edifício, a localização e a exposição ao ambiente externo. Finalmente, uma tentativa é feita para extrapolar as descobertas para todas as tipologias de escritórios da Grécia. A partir desse ponto, utilizando o sistema de aquecimento de energia solar ativo proposto, a economia de energia térmica alcançaria 29% no total devido à cobertura solar.

Palavras-chave: Coletores solares. Aquecimento de escritórios. ESP-r.

Abstract

This paper explores the feasibility of using solar thermal collector systems with storage capacity and conventional radiators to support space-heating applications of office buildings in Greece. A dynamic simulation model in ESP-r tool is employed to analyze the performance of the building-integrated solar collector system for different demand profiles in all the climatic zones of Greece. The impact of the storage system capacity, the collector area and the tilt angle were investigated as to what extend the overall system performance is influenced. The offices in Greece are approximated within various yearly demand scenarios, determined by the building orientation, the location and the exposure to the outer environment. From that point, using the proposed active solar space heating system, further thermal energy savings of 29 % are achievable in total due to solar coverage.

Keywords: Solar thermal collector. Office heating. ESP-r.

1 Introduction

Solar thermal systems are used nowadays for a wide range of applications; domestic hot water (DHW), swimming pools heating, space heating (SH), district heat, process heat, solar cooling and electricity production from solar thermal power plants (Streicher, 2016). Capturing free energy from the sun, these systems generate low-cost and environmentally friendly thermal energy. While solar energy markets have been established worldwide over the past decades (STREICHER, 2016), particularly Mediterranean countries of southern Europe, have come up with very well developed solar thermal markets (ESTIF, 2014), managing to take advantage of their high levels of solar irradiation (OME, 2012).

Focusing on Greece, solar thermal collectors have been popular mostly for domestic applications for hot water provision systems. The main solar thermal product in the country has been the thermosiphon water heater. Greece's solar thermal market has been active for well above 30 years, allowing the country to have one of the highest solar thermal capacities within Europe for many years (GIAKOUMI; IATRIDIS, 2009).

Giakoumi and Iatridis (2009) also state that domestic hot water (DHW) production constitutes the impressive 98 % of the total installed solar thermal collector area in Greece. On the other hand, little consideration has been given to the utilization of the solar thermal technology for space heating (SH), which comprised not nearly as much as 1% of the installed collector area in the country in 2009.

Moreover, according to the general trend in Greece, Renewable Energy Sources (RES) have been mostly associated with the electricity generation rather than the heating sector. Thusly, apart from the hot water supply, for which the solar integration was at 31.4 % in 2004 among other sources, space heating in Greece is basically provided by non-RES with negligible solar integration (GIAKOUMI; IATRIDIS, 2009).

There has been a number of independent studies on the development of active solar space heating systems for different countries worldwide. The design of an experimental solar energy facility for Spanish housing (MARCOS; IZQUIERDO; PARRA, 2011) as well as the TRNSYS model-based sensitivity analysis of a solar heating system for a Greek multi-storey building (STEGOU-SAGIA; KORONAKI; SAGIA, 2010) have made considerable efforts to assess the applicability and viability of active solar thermal technology for Mediterranean countries.

However, as depicted from the lack of sufficient data in the national statistics services of Greece, as well as from the absence of relevant policy schemes for the support of the renewables heating sector (GIAKOUMI; IATRIDIS, 2009), it is apparent that the focus has remained on electricity rather than the heating from RES. This partly explains why the results of the above and other relevant works on solar heating systems (SOBHY; BRAKEZ; BENHAMOU, 2015) have not been applied to a greater extend for the case of Greece.

Among the lack of policies, plans and programmes to support solar space heating applications, financial barriers have also restrained the growth of this sector in Greece. During a time when the aftermath of the financial crisis has strongly affected Greek economy, initial capital cost investments as well as potential increased maintenance requirements have deterred people from replacing old heating systems with new ones. While high investment costs compared to conventional systems are common to most renewable energy technologies (OME, 2012), additionally there are technical difficulties that arise regarding solar space heating, for example when it comes to refurbishing older buildings and integrating underfloor heating systems. In each case, specific incentive programmes need to be implemented in order to reduce the gap between the solar thermal and the traditional technologies and help overcome the aforementioned financial and technical barriers (OME, 2012).

The overall aim of the paper is to evaluate the technical feasibility and assess the energy and environmental performance of active solar thermal technology with storage capacity and conventional radiators for space heating applications to the office buildings in Greece.

2 Methodology

The methodology is composed of the following key steps to be followed throughout the project:

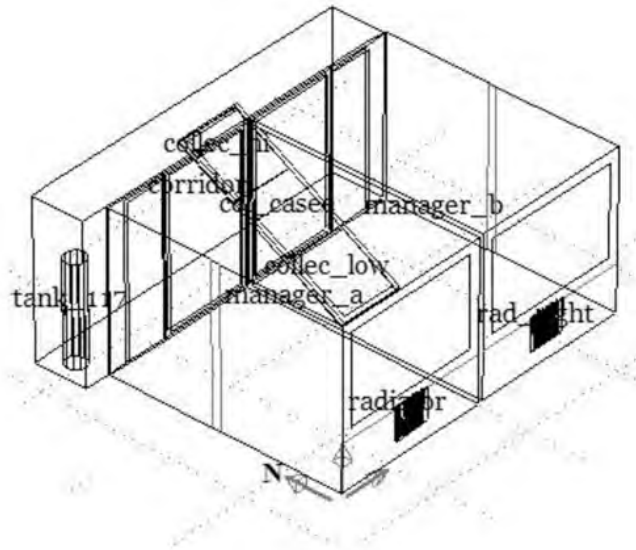
- ◆ Use a building model and adjust it to describe a typical office/commercial application for solar space heating in Greece. ESP-r software is a useful tool for simulating the building-integrated active solar space heating system through dynamic modelling, as analysed later.
- ◆ Investigate how the selected active solar system performs in different building orientations, climatic zones and structural exposures, resulting in final “average” energy performance for each climatic zone.
- ◆ Extrapolate the “average” energy performance to the whole office/commercial building stock of Greece, so that the energy and environmental performance is ultimately appraised. Thermal energy savings result for the whole country, as well as for each climatic zone separately, as regards the offices, as part of the non-residential sector.

2.1 Dynamic Modelling Tool (ESP-r)

The modelling tool that has been selected for the simulation of active solar space heating systems for this research project is ESP-r, an integrated building/plant simulation tool. It is appropriate for modelling building performance and undertaking

energy assessments, regarding heat, airflow, water flow, light and electrical calculations (ESRU, n.d.).

Figure 01. ESP-r model *cellular_expl_sdhw* of two adjacent cellular offices with zone-based SDHW



Source: GitHub, 2016.

One of the absolute benefits of ESP-r tool that particularly fits this project is its suitability for the design of a building-integrated system, while all modelled elements mentioned above are possible to be incorporated into the same building domain. This holistic approach allows the well-informed user to be able to make improvements to the building model, taking advantage of the software's range to features and performing an in-depth appraisal of the factors which affect the energy and environmental performance of the building. Its flexibility in building modelling make ESP-r a powerful tool for research purposes like this, in addition to uses in teaching and consultancy contexts (ESRU, n.d.).

3 Design of the model

The model in ESP-r includes two adjacent offices, connected with a corridor, featuring an active solar water system for space heating. It incorporates a water-based solar collector, an insulated hot water storage tank, which is located in the left corner of the corridor zone, and two water filled radiators, one in each office (GitHub, 2016). In addition to the water filled zones, there are also separate air filled zones to represent the two offices, the corridor and the collector case. In total, there are ten different zones defined in the model, as shown in Table 1. This model is referred to as *cellular_expl_sdhw* from now on.

Table 1. Breakdown of zones defined in ESP-r model *cellular_expl_sdhw*

	#	Zone name	Zone description
Air filled zones	1	manager_a	Office A
	2	manager_b	Office B
	3	Corridor	Corridor between the two offices
	4	col_casee	Collector case/housing
Water filled zones	5	collec_low	Lower part of solar collector
	6	collec_mid	Middle part of solar collector
	7	collec_hi	Higher part of solar collector
	8	tank_117	Storage tank
	9	Radiator	Radiator in office A
	10	rad_right	Radiator in office B

Source: GitHub, 2016.

The model initially incorporates a solar collector area of 4.32 m² and a storage tank capacity of 205.2 L, while the tilt angle is adjusted at 30° from horizontal. The capacity of each radiator is around 8 L of water.

The nodes of the active solar system in the model are connected through the components of the flow network. The collector pump is placed in line with the solar loop, between the nodes of *collec_low* and *tank*, while the rest of the solar circuit is realised with conduit linkages between the *collec_low*, *collec_mid*, *collec_hi* and *tank* nodes. A similar realisation is achieved in the radiator loops, where each of the radiator pumps is placed between the *tank* and each of the radiators of the offices.

When the top of the solar collector (*collec_hi*) is 3 °C warmer than the storage tank temperature, the collector pump in the solar loop is activated. Nevertheless, each of the radiator pumps is kept on as long as the temperature of the respective office is below 22 °C, regardless of the storage tank temperature. Moreover, a very low flow (trickle) circulator is operating between the *tank* and the collector to reduce extreme conditions in the latter (GitHub, 2016).

The *cellular_expl_sdhw* model is compared to an identical building model except the inclusion of the active solar system, which constitutes the basis for the comparisons in the current work. This is the base case model of two adjacent cellular offices, referred to as *cellular_bc* (GitHub, 2016).

The base case model has to be exactly the same to the main model used for the active solar space heating (*cellular_expl_sdhw*), which means they both have the same office dimensions, window sizes, construction materials, ideal controls and operational details, namely same casual gains and scheduled air flows. The only differentiation of the *cellular_bc* model is the absence of the active solar system. Therefore, the amount of energy calculated from the *cellular_expl_sdhw* model is equal to the energy that

needs to be provided from the conventional heating system of the office to complement the active solar system operation. As a result, it is valid to calculate the actual amount of energy delivered from the active solar system, by estimating the difference of the delivered energy between the two models.

4.1 Dimensioning and geometry

The typical office building represented by the model in ESP-r incorporates two adjacent office rooms linked together with a corridor at one side and having large windows at the opposite side for exploiting daylight harvesting.

It is important to point out that the corridor in the model represents a small walking hall/passage leading to the offices and it does not assume part of the heating system. Furthermore, in the cellular_expl_sdhw model the corridor offers the space for the hot water storage tank, as part of the active solar heating system. However, the focus regarding the heating demands is maintained on the two office rooms, rather than the corridor, which underlies to free floating conditions.

The active solar heating system consists of three basic elements represented by thermal zones in the model; the solar collector, the storage tank and the radiators. Before presenting the geometry characteristics of these basic features, it is important to understand their structure and correspondence to thermal zones.

The solar collector is composed of four parts which correspond to four different thermal zones defined in the model; col_casee (collector casing), collec_low (lower part of the panel), collec_mid (middle part of the panel) and collec_hi (top part of the panel). The initial value of the total collector area is set at: 4.32 m^2 which occupies nearly $4.32 \text{ m}^2 / (13.5 + 13.5) \text{ m}^2 = 16\%$ of the equivalent to the offices roof space area. The dimensions and the resulting area of the collector plates in the model are shown in Table 2 below.

Table 2. Collector plates dimensions and resulting collector area in the model (initially)

Collector plates	Dimensions (m)	Area (m ²)	Total collector area	Roof space coverage
collec_low	1.2 x 1.2	1.44	4.32 m ²	16 %
collec_mid	1.2 x 1.2	1.44		
collec_hi	1.2 x 1.2	1.44		

Source: Author, 2016.

As far as the volumes of the collector elements is concerned, each of the collector plates has initially a volume of 14 L (water filled zones), while the volume of the collector case in the model is equal to 432 L (air filled zone). This results from the collector case having a width of 0.1 m over its surface area of 4.32 m^2 .

The storage tank for the hot water in the model is approximated as a cylindrical structure, located inside the corridor zone. At the initial design stage of the active solar thermal system, the volume of the tank in the model is equal to 205.2 L, resulting from a base/floor area of 0.108 m² and a height of $2 - 0.1 = 1.9$ m. Its opaque construction area is equal to around 2.46 m².

Lastly, the radiators of the heating system installation in ESP-r model are located inside each of the office rooms and are identical to each other. The dimensions of the radiator are 0.7 m x 0.6 m, while the maximum width reaches 0.05 m, since there are several slots to increase the heat exchange area, as appeared in Figure 15 below. Its capacity is nearly 8 L of water, deriving from a base/floor area of 0.013 m² and its height of 0.6 m as mentioned above. Finally, its opaque construction area is equal to 1.08 m², which corresponds to the heat transfer area between the water inside the radiator and the air of the office room.

4.2 Construction materials

Both models (*cellular_bc*, *cellular_expl_sdhw*) have been adjusted so as to have the same construction materials. The offices feature double glazing windows, insulated spandrel as well as insulated window frames on the façade. The spandrel in the models is the façade surface below each of the windows.

The double glazing windows have an overall thickness of 24 mm and a total horizontal U-value of 2.811 W/(m²K). They consist of three layers in total, two layers of plate glass with air gap insulation between them.

Both the spandrel and the window frame, which are elements of the façade, are composed of insulation frame with overall thickness of 88 mm and a total horizontal U-value of 0.461 W/(m²K). Two layers of grey coated aluminum are separated with glass fiber insulation in between.

The rest of the office walls are composed of two layers of gypsum board partitions with air gap insulation in between. The overall thickness of the wall is 74 mm and the horizontal U-value is 2.144 W/(m²K).

As regards the active solar system construction materials, firstly the collector plates are composed of black coated copper, suitable for the effective absorption of the solar thermal energy.

Secondly, the collector case frame providing insulation to the back and the sides of the panels is composed of the same insulation frame materials, grey coated aluminum layers are separated with glass fiber insulation, resulting in a total U-value of 0.461 W/(m²K). The transparent covering of the panels is consisted of single glazing clear float glass, the U-value of the single glazing is equal to 5.691 W/(m²K).

Moreover, the base, top and all side surfaces of the storage tank are consisted of three layers, having Urea-formaldehyde foam insulation between the external (steel)

and internal (copper) layer. The overall horizontal U-value of the surfaces here is equal to $0.748 \text{ W}/(\text{m}^2\text{K})$.

Lastly, the radiators are made of white painted steel (3 mm), as the external layer in Table 16 above, having a horizontal U-value of $5.880 \text{ W}/(\text{m}^2\text{K})$. This relatively high U-value is important for the effective thermal exchange between the surface of the radiators and the air inside the office rooms.

4.3 Operational details

The operational details of the model include the casual gains from occupants, lighting and equipment, as well as the scheduled air flows.

Standard occupancy patterns for both offices and the corridor have been used according to the day type, namely weekday, Saturday or Sunday. This represents a typical occupancy pattern, similar to the quoted patterns in relevant works for office buildings (DUARTE et al., 2013). Between 09:00- 12:00 and 14:00-17:00 the maximum amount of heat gains is coming from almost two people in average inside each office, while typically there is one person at each office most of the time.

Lights operate in both the offices and the corridor, while gains from equipment are considered in the offices zones only. During a typical weekday in each office, the profile of casual gains from lighting is specifically, between 08:00-18:00, each of the lighting and equipment gain is set at $5 \text{ W}/\text{m}^2$, or 67.5 W for each office.

As regards the scheduled air flows, the values of the infiltration rates are adjusted, which in ESP-r account for the air movement and exchanges with the outside. Whether unintentional or mechanically forced, the air exchanges with the outside of the building are necessary for the proper ventilation of the inside space and must be taken into account in the model since they directly affect the heating demands.

The infiltration rates in our model are set at 0.33 air changes per hour (ac/h) for each office. This means that ESP-r accounts for fresh air entering each office zone (volume = 40.5 m^3) at a rate of: $(0.33 \text{ ac/h}) \cdot (40.5 \text{ m}^3) = 13.365 \text{ m}^3/\text{h} \approx 3.7 \text{ L/s}$

This infiltration rate is considered sufficient for limiting CO₂ concentration levels to 0.5% for two people working inside the office performing “light work” (office work) according to CIBSE standards for acceptable indoor air quality (CIBSE, 2001).

4.4 Surface connections and boundary conditions

The level of exposure of the office to the outer environment can be adjusted in the model from the connections between surfaces which determine the boundary conditions of the zones. Initially, our case study includes an office as part of a block of offices, which generally represents a *low demand* case for Greece. This is the reason why the floors of the offices are set to be connected with an identical environment on

the respective lower floor of the building. The well-insulated ceilings are set as external. However, it is considered that one of the offices is internal from both sides and the back, having only its façade exposed to the outer environment, while the other office has one side exposed as well as its façade.

4.5 Control loops

The model uses one control loop to heat up the two offices. The control loop represents the conventional auxiliary heating system, which is responsible for keeping the temperature inside the offices at the desired level, regardless of the solar source availability. This means that the auxiliary system will be in operation for as long as it is needed in order to provide adequate heating load for the building to reach the set temperature, while complementing the operation of the active solar system.

The control loop is linked to zones manager_a and manager_b, namely to the two offices, which constitute the main space that needs to be heated up in our model. The total floor area for which space heating is required is 27 m². Heating load is requested at regular office hours on weekdays and reduced hours on Saturdays. Finally, on Sundays the auxiliary heating system is on stand-by and it is set at a low reference temperature.

The sensor for the control loop senses the current zone dry bulb temperature, while the actuator is located at the air point of the respective zone featuring a purely convective injection of heat.

4.6 Integrated simulation parameters

The integrated simulation of the *cellular_expl_sdhw* model needs to run interactively, while adjusting the simulation toggles accordingly. The non-air filled zones, namely the water filled, need to be selected and then the following properties of the fluid, which is water in this case, are entered:

Thermal Conductivity: $k = 0.598 \text{ W/(mK)}$ (at 20 °C)

Density: $\rho = 998 \text{ kg/m}^3$ (at 20 °C)

Specific Heat: $c_p = 4182 \text{ J/(kgK)}$ (at 20 °C)

Absorptivity: $\alpha = 0$

The mass flow stack pressure method value (IPSMOD) needs to be changed from 1 (sending node) to 2 (average of nodes). Afterwards, the mass flow parameters need to be reentered. More specifically, there is a number of parameters, which control the iterative fluid flows calculation process (GitHub, 2016).

4.7 Climatic data

There are four climatic zones in the Greek territory, according to the legislation scheme KENAK (YPEKA, 2010). The key was to find available weather data for each region, which could be representative of the respective climatic zone. Four different cities in Greece have been chosen to represent each climatic zone, as appeared in Figure 02:

Figure 02. Location of simulated climates in Greece



Source: Papamanolis, 2015.

The weather data for Athens and Thessaloniki have been available on EnergyPlus website (ENERGYPLUS, n.d.) and for Kastoria and Iraklion in Meteonorm weather files category at the EnergyPlus Support yahoo group (ENERGYPLUS SUPPORT, 2016).

There are significant differences in the climatic characteristics between the climatic zones. As stated in the “Climatic Data of regions in Greece” technical directive (TEE, 2012), regions are classified into climatic zones from the warmest to the coldest, following the order from zone A to D.

However, the order of climatic zones from warmer to colder is not straight forwardly correlated with the mean values of the direct solar radiation, as can be seen in Table 3. Although these values are reduced from zone A to C, a very interesting differentiation from this pattern occurs for the coldest zone D. The fact that Kastoria area (zone D), albeit the coldest, has higher mean direct solar radiation even from

Athens (zone B) can lead to very interesting results regarding the performance of the active solar thermal system there.

Table 3. Yearly stats for climatic characteristics in each area

City	Climatic Zone	Year of data	Dry bulb temperature (°C)			Direct normal radiation (W/m ²)		
			Min	Max	Mean	Min	Max	Mean
Iraklion	A	2005	5.1	35.7	18.6	0	982	217.3
Athens	B	1999	2	37.2	17.9	0	942	173.1
Thessaloniki	C	1984	- 4.2	34.8	15.3	0	894	156.8
Kastoria	D	2005	- 8.9	39.2	12.8	0	1025	193.2

Source: Author, 2016.

5 Initial design of the model

The heating demand loads predicted from the building-integrated simulations of the two models, using the initial design are summarised in Table 4. The estimations of the models concern the yearly energy delivered from the heating control loops in ESP-r, which represents the delivered energy from the conventional heating system of the offices.

Initial Scenario:

4.32 m² collector area (16% roof space) 30° tilt angle
 205.2 L tank (47.5 L/m²) Kastoria (Zone D)

Table 4. Yearly heating demands for the two offices in Kastoria before and after the implementation of the active solar system

Model	Heating energy (kWh)	Specific heating energy (kWh/m ² a)	Total heating hours
Cellular_bc	Q _{total} = 1115.7	41.32	3702
Cellular_expl_sdhw	Q _{aux} = 718.6	21.61	2844

Source: Author, 2016.

The base case heating demands deriving from the *cellular_bc* model for Kastoria, having all constructional and operational details as described, are equal to 1115.7 kWh annually or 41.32 kWh/m²a, considering the total heating area of 27 m² of the two offices where the heating control loops apply.

This value represents a generally *low demand* office building profile for the climate of Kastoria (Zone D). It constitutes an average low demand base case, which includes one office internal from both sides and one office external from the one side, while both are part of an office block and they both have external façades. According to the difference from the heating control loop calculations between the two described models, the active solar system in this case contributes to around $1115.7 - 718.6 = 397.1$ kWh annually, which is interpreted as a solar coverage fraction of $397.1 / 1115.7 \approx 35.6\%$.

Alternatively, using the equation:

$$\text{Solar fraction} = 1 - 718.6 / 1115.7 \approx 35.6\%$$

This means that the implementation of the initial scenario for the active solar system in Kastoria leads to potential annual thermal energy savings of around 35.6%. This results in a final specific thermal energy demand of 26.61 kWh/m²a, which is a significant improvement for the *low demand* office building in Kastoria. This improvement is also depicted in the total number of required heating hours for the two offices yearly, which is reduced by $1 - 2844 / 3702 \approx 23.2\%$. It is important to note that the number of total heating hours refers to the sum of the heating hours required for each office, even if some of these coincide.

The breakdown of the monthly total heating demand (Q_{total}) for the two offices in Kastoria, as well as the monthly residual heating demand (Q_{aux}) after the implementation of the active solar system, are presented in Table 5 for the initial scenario, resulting from the simulations of the models *cellular_bc* and *cellular_expl_sdhw* respectively. Consequently, the solar coverage fraction is estimated on a monthly basis as well, using the same equation mentioned before.

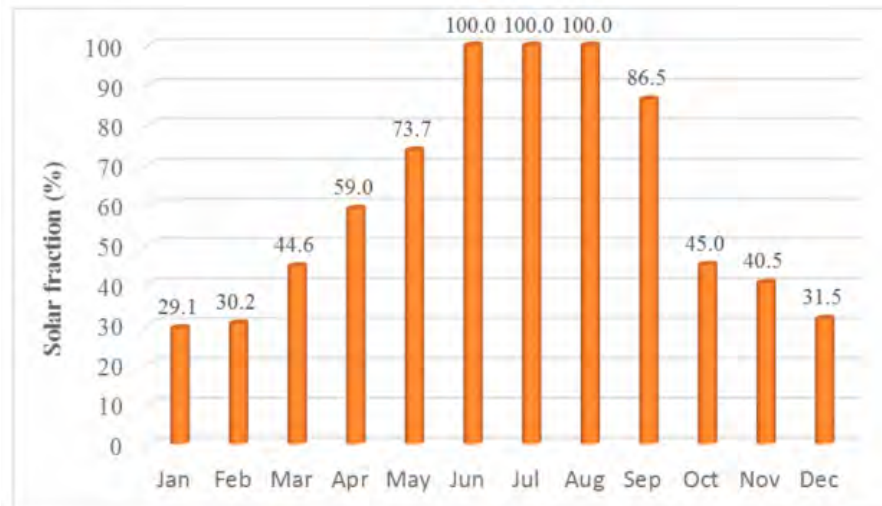
Table 5. Monthly and annual simulated demands and solar fractions for the two offices in Kastoria for the initial scenario

Kastoria	Q_{total} (kWh)	Q_{aux} (kWh)	Solar fraction (%)
January	289.9	205.6	29.1
February	225.5	157.3	30.2
March	152.6	84.5	44.6
April	53.7	22	59.0
May	7.6	2	73.7
June	0.6	0	100
July	0.1	0	100
August	0	0	100
September	3.7	0.5	86.5
October	27.8	15.3	45.0
November	125.7	74.8	40.5
December	228.5	156.6	31.5
Year	1115.7	718.6	35.6 %

Source: Author, 2016.

As can be observed in Table 5, the solar fraction is the lowest in the coldest month of the year (January) and thereafter becomes higher as moving toward the summer months, where the heating demands are negligible, leading to 100% solar coverage by any means. Afterwards, the solar coverage percentages are reduced as approaching to the winter, with December however having a higher solar fraction than January and February. This described trend appears better in Figure 3 below.

Figure 3. Monthly solar fractions for the initial scenario in Kastoria



Source: Author, 2016.

Thence, the analysis of the model is carried out, regarding its sensitivity to the parameters of the active solar system. The model is tested for different values of the initial design parameters, consecutively the specific storage tank size (storage volume per m^2 of collector area), the collector area and the tilt angle, so as for the impact of these parameters on the model to be assessed. During each step, the final value of the respective parameter is decided, resulting in the final selection of the active solar system which will afterwards be used for the whole office building stock of Greece.

3.2 Impact of specific storage tank volume

Based on the initial scenario, the collector area of 4.32 m^2 (16% roof space) is kept stable while changing the specific storage volume downwards and upwards from the initial value of 47.5 L/m^2 of collector area. Hence, two scenarios come up with a specific storage volume of 22.5 L/m^2 and 70 L/m^2 respectively. The resulting absolute storage volumes of 97.2 L and 302.4 L are implemented into the model by setting the height in all vertices of the top surface of the tank to 1 m and 2.9 m respectively. The second case leaves enough space to accommodate the insulation of the top surface of the tank under the ceiling (height = 3 m).

Consequently, the simulated scenarios and the results comparison with the initial scenario, while changing the specific storage tank volume, turn up as follows:

Scenario 2:

4.32 m² collector area (16% roof space) 30° tilt angle
 97.2 L tank (22.5 L/m²) Kastoria (Zone D)

Scenario 3:

4.32 m² collector area (16% roof space) 30° tilt angle
 302.4 L tank (70 L/m²) Kastoria (Zone D)

Table 6. Yearly simulated results comparison with different specific storage tank volumes

Kastoria (Zone D)	Tank Volume (L/m ²)	Qtotal		Qaux		Solar Fraction	Solar Fraction difference
		kWh	kWhm ² a	kWh	kWhm ² a		
Initial Scenario	47.5	1115.7	41.32	718.6	26.61	35.6%	0%
Scenario 2	22.5	1115.7	41.32	743.6	27.54	33.4%	-2.2%
Scenario 3	70	1115.7	41.32	693.6	25.69	37.8%	+2.2%

Source: Author, 2016.

As can be observed from the yearly simulations with variable specific storage tank volume, there is a fair impact of the storage size on the building-integrated active solar system performance. It was anticipated that the yearly solar coverage fraction increases as the specific storage size increases.

The same occurs with the monthly solar fractions, where the impact of changes is higher during the autumn and spring months and slightly lower during the winter months. During the summer months, the heating demands of the office building are negligible by any means, so that the solar coverage fraction from almost all systems reaches 100%.

3.4 Impact of collector area with standard specific storage size

The testing of the model continues as regards the impact the solar collector area has on its energy performance. After concluding to a specific storage volume of 70 L/m² of collector area, it is apparent that the changes in the collector area are also reflected to changes in the storage capacity of the system. Basically, within the active solar system, the pair of the collector area and the storage tank size is considered as a “subsystem”, the capacity of which affects the performance of the total building-integrated system.

Two different collector areas are tested at 2.16 m² (8% of the roof space coverage) and at 3.24 m² (12% of roof space), featuring a storage volume of 151.2 L and 226.8 L respectively (70 L/m²). Hence, the following scenarios come up with the simulation results comparison between them and the scenario 3 indicating the impact of changes:

Scenario 4:

2.16 m² collector area (8% roof space) 30° tilt angle
 151.2 L tank (70 L/m²) Kastoria (Zone D)

Scenario 5:

3.24 m² collector area (12% roof space) 30° tilt angle
 226.8 L tank (70 L/m²) Kastoria (Zone D)

Table 7. Yearly simulated results comparison with different combinations of collector area – tank size (70 L/m²)

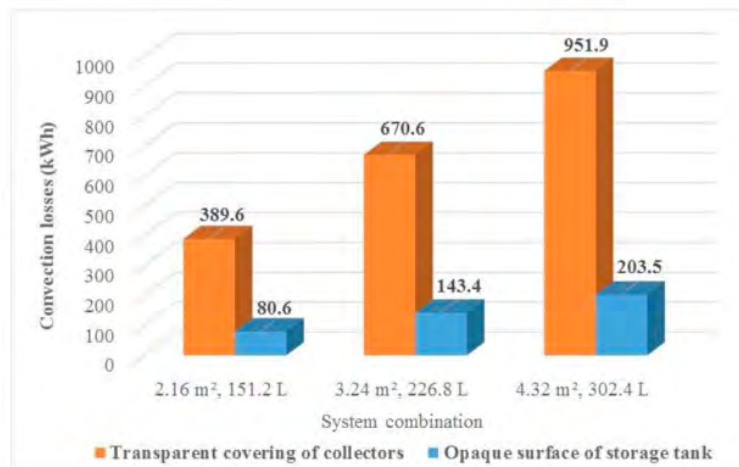
Kastoria (Zone D)	Colle area (m ²)	Storage volume (L/m ²)	Q _{total}		Q _{aux}		Solar	Solar Fraction
			kWh	kWhm ² a	kWh	kWhm ² a		
Scen. 3	2.16	151.2	1115.7	41.32	740.9	27.44	33.6%	0%
Scen. 4	3.24	226.8	1115.7	41.32	709.8	26.29	36.4%	+ 2.8%
Scen. 5	4.32	302.4	1115.7	41.32	693.6	25.69	37.8%	+ 4.2%

Source: Author, 2016.

As can be derived from the results in Table 7, there is an anticipated impact of the combination collector area – storage tank volume on the energy performance of the building-integrated active solar system. The yearly as well as the monthly solar coverage fraction increases as both the collector area and the storage volume increase in magnitude. As regards the monthly increases, there is a clearer impact of the larger system during the spring and autumn months than the winter months. From the summer months, only in June the solar fraction does not reach 100% with the two smaller systems, albeit remaining above 90%.

The fact that the impact of the applied system alterations is not extensive to the final energy performance can be explained by taking a look at the energy losses of the system. It is known that energy losses occur in almost every part of the system; the transparent covering (glazing) of the collectors, the sides and back of the collector case, the tubes, the storage tank surfaces are some examples of particular areas where heat losses can occur. In Figure 4, the yearly convective losses through the transparent covering of the panels to the outside and through the opaque surface of the storage tank is depicted for the three tested system combinations.

Figure 4. Yearly convection losses through transparent covering (glazing) of collectors and through opaque surface of tank with different combinations of collector area – tank size (70 L/m^2)



Source: Author, 2016.

This analysis shows that the energy losses of the system, as calculated by the model, increase disproportionately with the increase of the system capacity. This occurs because, in addition to increasing the thermal exchange surfaces, there is an increase of the temperatures in the collectors and the tank accordingly. The increased system losses eventually reduce the efficiency of the larger systems and can limit their energy performance. Although effort has been made to explain this behaviour of the system in the model, it is not within the scope of this study to reduce heat losses of larger systems. Given the behaviour of the system, it would be agreeable to select a system combination with reasonable energy performance and efficiency, at low cost and low space requirements.

Consequently, the combination of the 2.16 m^2 collector area, 151.2 L storage tank would be acceptable for the application to the office sector in Greece, in terms of its energy performance and the very low percentage (8%) of the roof space covered by the collectors.

If solar systems with similar proportions of collector area and storage size per m^2 of heated floor area (0.08 m^2 collector/ m^2 floor and 5.6 L/m^2 floor respectively) were to be applied massively within the office sector in Greece, significant fractional energy savings could result for the country. At the same time, this choice offers low space requirements, in terms of both roof space coverage and storage capacity, which could make it technically applicable to a greater extend in the Greek offices.

3.5 Impact of collector tilt angle

After selecting the collector area and the storage tank size of the active solar system, one very important aspect to be considered is the tilt angle of the solar

collectors. The initial design of the system features solar collectors tilted at 30° from horizontal. Changing the tilt angle of the panels inside the model is a procedure that requires accurate trigonometric calculations to determine the final coordinates of all the vertices of the zones collec_low, collec_mid, collec_hi and col_casee after tilting the panel by the desired angle. Moreover, the respective flow network nodes need to be updated, especially regarding their reference height attributes to support buoyancy calculations in the programme.

The studied scenarios include the selected system combination (2.16 m² collector area, 151.2 L storage volume) with the solar collectors tilted at 40° and 50° from horizontal consecutively, and the simulated results are compared as follows:

Scenario 6:

2.16 m² collector area (8% roof space) 40° tilt angle
151.2 L tank (70 L/m²) Kastoria (Zone D)

Scenario 7:

2.16 m² collector area (8% roof space) 50° tilt angle
151.2 L tank (70 L/m²) Kastoria (Zone D)

Table 8. Yearly simulated results comparison with different tilt angles

	Kastoria (Zone D)	Q _{total}		Q _{aux}		Solar Fraction	Solar Fraction difference
		kWh	kWhm ² a	kWh	kWhm ² a		
Scen. 5	2.16 m ² , 151.2 L, 30°	1115.7	41.32	740.9	27.44	33.6%	0%
Scen. 6	2.16 m ² , 151.2 L, 40°	1115.7	41.32	710.6	26.32	36.3%	+ 2.7%
Scen. 7	2.16 m ² , 151.2 L, 50°	1115.7	41.32	680.1	25.19	39.0%	+ 5.4%

Source: Author, 2016.

The results shown in Table 8 indicate the significant impact the tilt angle of collectors has on the active solar system energy performance. Indeed, the impact of tilt angle alterations is noticeable, especially comparing with the impact the previous changes had on the system. The yearly performance improves from 30° to 40° and, subsequently, from 40° to 50° tilt angle from horizontal. It is remarkable that the (2.16 m², 151.2 L) system with a 50° angle can reach a yearly solar fraction percentage (39 %) in Kastoria, which could not be achieved even when applying a larger system with the previous tilt angle (30°). This indicates how powerful tool is the inclination angle when installing solar collectors, which could lead to cost- and space-effective solutions, instead of applying a larger system capacity.

The whole set of model tests has been carried out for the climatic zone D of Greece, represented by the weather of Kastoria. This zone features colder climatic characteristics in comparison with the rest of the zones (TEE, 2012). The resulting solar system for this climate will have sufficient capacity for the rest of the country as well.

After all, the selected combination for the active solar system features 2.16 m^2 of collector area (8 % roof space coverage or $0.08 \text{ m}^2 \text{ collector/m}^2 \text{ floor}$), a storage tank capacity of 151.2 L (70 L/m^2 of collector area and $5.6 \text{ L/m}^2 \text{ floor}$) and a tilt angle for the collectors adjusted at 50° from horizontal.

According to the simulation results at this point, this system could be able to contribute to around 39 % of the yearly thermal energy required for space heating of the two offices in Kastoria. The rest 61 % needs to be provided by the conventional (auxiliary) heating system already installed in the offices.

4 Conclusions

To sum up, the installation of a closed loop forced circulation active solar system with flat plate collectors, storage capacity and closed radiator heating loop, featuring:

- ♦ $0.08 \text{ m}^2 \text{ collector area} / \text{m}^2 \text{ heated floor area}$;
- ♦ $70 \text{ L storage volume} / \text{m}^2 \text{ of collector area}$ or $5.6 \text{ L storage volume} / \text{m}^2 \text{ heated floor area}$ and
- ♦ 50° tilt angle of collectors and south orientation (180° azimuth angle from north)

To the whole office building stock in Greece, of a total floor area of 25,544,135 m^2 would result in a total solar collector area of nearly 2.05 million m^2 and a storage capacity of roughly 143 million L in total.

Compared to the total surface of glazed collectors, which was already operating in Greece in 2007 and reached approximately 3.57 million m^2 (Giakoumi and Iatridis, 2009: 21), the present venture for the office buildings would require almost 57 % more collector area to be added to the existing throughout the country.

If this system was to be applied massively to the total office building sector throughout Greece, a number of buildings would firstly need to be subject to significant improvements (Energy Conservation Measures or ECMs) as proposed by Gaglia et al. (2007), such as thermal insulation of external walls and roofs, double glazing and a successful building management system over the heating and ventilation controls.

After these upgrades have been implemented to the Hellenic office building stock, the currently proposed active solar system would be able to be applied massively with considerable outcomes. It is important that this system, as simulated in this study, would not require any further improvements in the heating system of the office buildings, such as the installation of an underfloor or wall-integrated heating loop. On the contrary, it is proven that the integration within the existing radiator heating loop would be feasible and would lead to remarkable results.

References

- CIBSE. Guide B2 - Ventilation and Air Conditioning. London: CIBSE. 2001.
- DUARTE, C.; VAN DEN WYMELENBERG, K.; RIEGER, C. Revealing occupancy patterns in an office building through the use of occupancy sensor data. *ENERGY AND BUILDINGS*, 67, p. 587-595, 2013.
- ENERGYPLUS. Weather Data | EnergyPlus. [online]. (n.d.) Available at: <https://energyplus.net/weather>. Accessed: 1 Jul. 2016.
- ENERGYPLUS SUPPORT. Yahoo groups. [online]. 2016. Available at: https://beta.groups.yahoo.com/neo/groups/EnergyPlus_Support/info. Accessed: 2 Jul. 2016.
- ESRU. ESP-r. [online]. n.d. Available at: <http://www.esru.strath.ac.uk/Programs/ESP-r.htm>. Accessed: 15 Jun. 2016.
- ESTIF. Solar Thermal Markets in Europe. Trends and Market Statistics. Brussels: European Solar Thermal Industry Federation. 2014.
- GAGLIA, A.; BALARAS, C.; MIRASGEDIS, S.; GEORGOPOULOU, E.; SARAFIDIS, Y.; LALAS, D. Empirical assessment of the Hellenic non-residential building stock, energy consumption, emissions and potential energy savings. *Energy Conversion and Management*, v. 48, n. 4, p. 1160-1175, 2007.
- GIAKOUMI, A.; IATRIDIS, M. Current state of heating and cooling markets in Greece. Policy development for improving RES-H/C penetration in European Member States (RES-H Policy). CRES, Greece: Intelligent Energy Europe, 2009.
- GITHUB. Build software better, together. [online]. 2016. Available at: <https://github.com/>. Accessed 19 Jun. 2016.
- MARCOS, J.; IZQUIERDO, M.; PARRA, D. Solar space heating and cooling for Spanish housing: Potential energy savings and emissions reduction. *Solar Energy*, v. 85, n. 11, p. 2622-2641, 2011.
- OME. (2012). SOLAR THERMAL IN THE MEDITERRANEAN REGION. SOLAR THERMAL ACTION PLAN. Nanterre: Observatoire Méditerranéen de l'Energie.
- PAPAMANOLIS, N. The first indications of the effects of the new legislation concerning the energy performance of buildings on renewable energy applications in buildings in Greece. *International Journal of Sustainable Built Environment*, v. 4, n. 2, p. 391-399, 2015.
- SOBHY, I.; BRAKEZ, A.; BENHAMOU, B. **Dynamic modeling of thermal behavior of a solar floor heating system for a HAMMAM in Marrakech**. IEEE, 2015. doi: <https://doi.org/10.1109/IRSEC.2015.7455139>
- STEGOU-SAGIA, A.; KORONAKI, I.P.; SAGIA, Z. **A Solar Space Heating Plant for Greek Buildings with underfloor heating system**. Proceedings of 23rd International Conference on Efficiency, Cost, Optimisation, Simulation and Environmental Impact of Energy Systems. ECOS 2010, Lausanne (Ecole Polytechnique Federale de Lausanne), Switzerland. 2010.

STRACHAN, P. **ESP-r: Summary of Validation Studies**. Glasgow: ESRU, 2000.

STREICHER, W. Solar thermal technologies for domestic hot water preparation and space heating. In: STRYI-HIPP, G. ed. **Renewable heating and cooling**. Amsterdam: Elsevier, p. 9-39, 2016.

TEE. **Climatic Data of regions in Greece**. T.O.T.E.E. 20701-3/2010 (In Greek). 2012. Available at: http://helapco.gr/pdf/TOTEE_20701_3_Final_TEE_2nd.pdf

YPEKA. **KENAK – Greek Regulation for the Energy Efficiency of Buildings**. EK407/B/9.4.2010 (in Greek). 2010.